



# HHS Public Access

Author manuscript

*J Control Release*. Author manuscript; available in PMC 2019 March 10.

Published in final edited form as:

*J Control Release*. 2018 March 10; 273: 147–159. doi:10.1016/j.jconrel.2018.01.027.

## Tunable Degradation of Acetalated Dextran Microparticles Enables Controlled Vaccine Adjuvant and Antigen Delivery to Modulate Adaptive Immune Responses

Naihan Chen, Monica M. Johnson, Michael A. Collier, Matthew D. Gallovic, Eric M. Bachelder, and Kristy M. Ainslie\*

Division of Pharmacoengineering and Molecular Pharmaceutics, Eshelman School of Pharmacy, The University of North Carolina at Chapel Hill, USA

### Abstract

Subunit vaccines are often poorly immunogenic, and adjuvants and/or delivery vehicles, such as polymeric microparticles (MPs), can be used to enhance immune responses. MPs can also be used to understand cell activation kinetics and the significant impact antigen and adjuvant release has on adaptive immune responses. By controlling antigen and adjuvant release, we can determine if it is important to have precise temporal control over release of these elements to optimize the peak and duration of protective immunity and improve vaccine safety profiles. In order to study the effect of tunable adjuvant or antigen delivery on generation of adaptive immunity, we used acetalated dextran (Ace-DEX) MPs. Ace-DEX MPs were used because their tunable degradation can be controlled based on polymer cyclic acetal coverage (CAC). Ace-DEX MPs of varying degradation profiles were used to deliver murabutide or ovalbumin (OVA) as a model adjuvant or antigen, respectively. When murabutide was encapsulated within Ace-DEX MPs to test for controlled adjuvant delivery, fast-degrading MPs exhibited higher humoral and cellular responses *in vivo* at earlier time points, while slow-degrading MPs resulted in stronger responses at later time points. When OVA was encapsulated within Ace-DEX MPs to test for controlled antigen delivery, fast-degrading MPs induced greater antibody and cytokine production throughout the length of the experiment. This differential response suggests the need for distinct, flexible control over adjuvant or antigen delivery and its impact on immune response modulation.

### Graphical Abstract

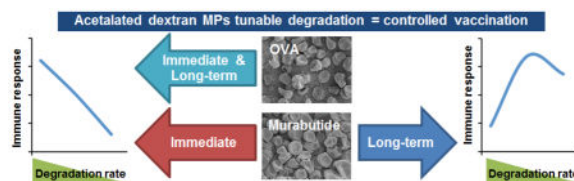
---

\*Corresponding Author: Kristy M. Ainslie, Associate Professor, UNC Eshelman School of Pharmacy, Division of Pharmacoengineering and Molecular Pharmaceutics, 4211 Marsico Hall, 125 Mason Farm Road, Chapel Hill, NC 27599, ainsliek@email.unc.edu.

#### Conflict of Interest

Drs. Ainslie and Bachelder serve on the advisory board for IMMvention Therapeutix, Inc. Although a financial conflict of interest was identified for management based on the overall scope of the project and its potential benefit to IMMvention Therapeutix, Inc., the research findings included in this publication may not necessarily related to the interests of IMMvention Therapeutix, Inc. The terms of this arrangement have been reviewed and approved by the University of North Carolina at Chapel Hill in accordance with its policy on objectivity in research.

**Publisher's Disclaimer:** This is a PDF file of an unedited manuscript that has been accepted for publication. As a service to our customers we are providing this early version of the manuscript. The manuscript will undergo copyediting, typesetting, and review of the resulting proof before it is published in its final citable form. Please note that during the production process errors may be discovered which could affect the content, and all legal disclaimers that apply to the journal pertain.



## Keywords

tunable delivery; microparticles; subunit vaccines; murabutide; electrospray; immune activation

## 1. Introduction

Vaccination represents one of the most potent and cost-effective public health practices for combating various infectious diseases and cancers. Traditional vaccines consist of live attenuated viruses, inactivated pathogens, or bacterial toxins [1]. Subunit vaccines are a safe alternative that utilizes surface proteins, peptides, or protein encoding nucleotides, which are much safer than the traditional vaccine approaches. However, poor immunogenicity of these well-defined antigens requires adjuvants and/or enhanced delivery systems to achieve optimal immune responses [2]. Aluminum salts (alum), the only FDA-approved adjuvant for decades until the recent development of MF59 and AS04 [3–5], promotes a robust humoral response, in part, through depot formation. Antigen adsorbed onto alum is released from the depot site for an extended period of time, allowing for long-lasting immune activation. However, alum offers little control over antigen release kinetics, generally fails to induce cytotoxic T-cell mediated (T helper 1 cells, Th1) immunity [6], generates local reactions, and has limited efficacy with some antigens [7]. Polymeric particles have been investigated by our lab [8] and others [9] as alternatives to alum with the objective to develop effective vaccines through efficient adjuvant or antigen delivery. Particulate vehicles can limit cargo degradation/denaturation, promote pharmacokinetic profiles, and allow for passive targeting to antigen presenting cells (APCs), if aptly sized [10, 11]. Prolonged and targeted adjuvant or antigen uptake by APCs enables sustained dendritic cell activation, which contributes to the enhanced immune response seen with particulate vaccine delivery [12] and has the potential to reduce dosage frequency and increase patient compliance.

Among all polymeric particulate delivery systems, poly(D,L-lactide-co-glycolic acid) (PLGA) is one of the most widely studied biodegradable polymers. PLGA composes many FDA-approved therapies and has been formulated into various particles for vaccine delivery [13]. However, PLGA generates acidic byproducts (lactic and glycolic acids) that can potentially lead to local cytotoxicity and can damage sensitive cargos [14–16]. Although efforts have been made to mitigate the pH shift by incorporating an antacid (e.g.  $Mg(OH)_2$ ) [17], other concerns such as slow degradation (half-life ranging from weeks to months) and limited tunability due to bulk erosion call for alternative delivery vehicles [18]. Because processes such as cell activation, antigen presentation, and cytokine production occur following a precisely controlled timeline that varies by different diseases [19, 20], the conventional vaccine delivery approach (i.e. uncontrolled release from the depot site) could significantly benefit from further control over the kinetics of antigen and adjuvant release in

the APCs [21, 22]. Understanding the kinetics of immune responses to vaccines is important in order to optimize the induction and duration of protective immunity, establish proper administration schedules for prime-boost vaccination [23], and design suitable delivery vehicles exhibiting optimal immune activation profiles for the disease of interest leading to better vaccine safety. Also, temporally controlled antigen delivery may optimize immune responses for specific diseases of interest since different antigen-APC interaction kinetics may lead to various downstream signals, which varies for distinct diseases [24, 25]. Therefore, alternative polymeric delivery systems need to be explored to achieve tunable adjuvant or antigen delivery *in vivo*, to optimize the peak and duration of protective immunity, to enhance efficacy and safety of subunit vaccines using a single formulation, and to improve our understandings of immune response kinetics post microparticle-mediated vaccination.

To address these challenges, acid-sensitive acetalated dextran (Ace-DEX) was used as an alternative material to formulate vehicles to achieve tunable vaccine delivery. With facile synthesis, pH-neutral hydrolytic byproducts, and passive targeting to APCs, Ace-DEX microparticles (MPs) have been previously investigated for various applications [26, 27]. Its stability outside cold chain storage adds another advantage to this system, where 70% bioactivity of an encapsulated enzyme was retained after 3-month storage at 25 °C or 45 °C [27]. When used for adjuvant delivery, Ace-DEX delivered polyinosinic:polycytidylic acid (poly I:C) and CpG more efficiently compared to PLGA [28]. When used for antigen delivery, Ace-DEX MPs promoted increased ovalbumin cross-presentation, compared to PLGA, in part due its acid-sensitivity [18, 29]. Synthesized from dextran with the hydroxyl groups replaced by acetals, Ace-DEX polymers can contain varying degrees of cyclic or acyclic acetal groups (i.e. cyclic acetal coverage, CAC). Based on the CAC and molecular weight (MW) of the starting material dextran, Ace-DEX MPs exhibit tunable degradation kinetics that can range from hours to months, with MPs of higher CAC degrading slower [30]. Considering the important role of temporal control over vaccine delivery in different diseases [23, 31], an Ace-DEX delivery platform with tunable degradation profiles may provide the opportunity to achieve controlled adjuvant or antigen delivery and tunable immune activation, contributing to optimal immune responses and the development of safer and more effective vaccines. Tunable degradation properties of Ace-DEX particles have been previously explored by Suarez et al. [32–34]. Using particles formulated with Ace-DEX of varying CAC, Suarez et al. optimized the release rate of cardioprotective molecules (e.g. myoglobin, basic fibroblast growth factor, and hepatocyte growth factor fragment) for myocardial infarction treatment. Suarez et al.'s research suggested the potential use of Ace-DEX MPs for controlled cargo delivery. Although other acid-labile carriers prepared from poly( $\beta$ -amino) esters (PBAEs), poly(ortho esters) (POEs), or polyketals have also demonstrated some flexibility in degradation kinetics [35–37], it is achieved mostly by varying polymer composition, which may result in complex manufacturing procedure and increased risk of adverse side effects associated with combining multiple biomaterials for controlled delivery [38]. These vehicles are also associated with other concerns: PBAEs may lead to severe side effects for long-term treatment due to potential toxicity [39, 40]; POEs are only stable under basic conditions and hydrolyze quickly in both acidic and neutral environments [41]; and, polyketals are synthesized via complex reactions, resulting in high

manufacturing cost and limited accessibility [42]. Therefore, Ace-DEX MPs represent a promising platform for efficient, flexible vaccine delivery. In our study, Ace-DEX MPs of different degradation profiles were prepared to study the kinetics of adjuvant or antigen delivery and characterize the control over immune activation post vaccination using a single formulation.

Using Ace-DEX MPs of varying CAC, we aim to characterize immune activation kinetics post vaccine delivery. To the best of our knowledge, we are among the first to examine tunable adjuvant or antigen delivery *in vivo*. Murabutide was selected to examine immune adjuvant response kinetics as it acts through intracellular nucleotide oligomerization domain (Nod)-like receptor 2 (Nod2) to activate the NF- $\kappa$ B signaling pathway [43–45]. Since murabutide does not readily permeate the cell membrane, intracellular delivery is required to achieve any substantial activity, which makes it an ideal adjuvant to study the intracellular degradation kinetics of Ace-DEX MPs and its effect on immune activation. Thus, encapsulated adjuvant (murabutide) and soluble antigen (ovalbumin, OVA) was selected to examine controlled adjuvant delivery. To study controlled antigen delivery, encapsulated antigen (OVA) and soluble adjuvant was selected. Toll-like receptor 4 agonist monophosphoryl lipid A (MPL) was selected as the soluble adjuvant for controlled antigen delivery, due to its extracellular signaling [46]. Electrohydrodynamic spraying (electrospray) was used to encapsulate murabutide or OVA to maximize compound loading and minimize protein denaturing during MP processing, compared to high-energy processes like emulsion [47, 48]. We characterized Ace-DEX MPs of varying CAC for their degradation kinetics under both neutral (pH 7.4) and acidic (pH 6.5) conditions and examined for various cargo release profiles. Adjuvant efficacy of murabutide-loaded MPs of different degradation rates was tested *in vitro* on JAWSII dendritic cells for cytokine production. To evaluate controlled adjuvant delivery, murabutide MPs were co-delivered with soluble OVA, and the kinetics of humoral and cellular responses were determined *in vivo*. In order to evaluate controlled antigen delivery, we investigated the magnitude and kinetics of antibody and cellular immune responses to OVA-containing MPs of varying CAC, co-delivered with soluble MPL. Immunity kinetics were characterized over a 6-week period by measuring serum antibody titers and splenocyte cytokine expression from multiple cohorts of vaccinated mice. Precise temporal control over vaccine release and immune activation can potentially allow for both rapid and sustained immune responses using a single delivery platform, contributing to our understanding of immune response kinetics post vaccination, and inspiring the development of safer and more effective vaccines for various diseases of interest.

## 2. Materials and Methods

### 2.1. Materials

All reagents were purchased and used as received from Sigma-Aldrich (St. Louis, MO) unless otherwise noted. Murabutide, ovalbumin (OVA, Ovalbumin EndoFit), OVA<sub>257–264</sub>, and synthetic monophosphoryl lipid A (MPL) were purchased from InvivoGen (San Diego, CA). Vaccine adjuvant Alhydrogel (Invivogen) was a generous gift given by Dr. Jenny Ting (Department of Microbiology and Immunology, University of North Carolina at Chapel Hill). Triethylamine (TEA) (0.01% v/v) was added to purified water (Millipore Milli-Q

Integral Water Purification System, Billerica, MA) to achieve a pH level of 9.0 (basic water) in presence of acetal-containing materials.

## 2.2. Cell culture

JAWSII (ATCC CRL-11904) dendritic cells were maintained following the manufacturer's protocol. This cell line was a kind gift of Dr. Jenny Ting. Cells were cultured in minimum essential medium (Fischer Scientific, Pittsburgh, PA) with ribonucleosides, deoxyribonucleosides, L-glutamine (4 mM), sodium pyruvate (1 mM), 20% fetal bovine serum (Hyclone, Pittsburgh, PA), 1% penicillin-streptomycin (Fischer Scientific, Pittsburgh, PA), and murine GM-CSF (5 ng/mL; Peprotech, Rocky Hill, NJ) at 37 °C with 5% CO<sub>2</sub> and 100% relative humidity.

## 2.3. Synthesis of acetalated dextran and analysis of relative cyclic acetal coverage

Ace-DEX was synthesized from 71 kDa dextran according to Chen et al. [49]. Dextran reacted with 2-ethoxypropene (Brookview Scientific, LLC, Carmel, IN) for 4, 20, or 1440 min to obtain low, medium, and high CAC as determined by <sup>1</sup>H nuclear magnetic resonance (NMR) spectroscopy. Ace-DEX polymer with low (19–21%), medium (38–41%), or high (59–62%) CAC will be referred to as Ace-DEX (20%), Ace-DEX (40%), or Ace-DEX (60%) for simplicity in this manuscript.

## 2.4. Fabrication of empty, murabutide-, or protein-loaded microparticles via electrospray

Ace-DEX MPs were prepared using the electrospray apparatus based on a protocol modified from Gallovic et al. [8]. Ace-DEX polymer was dissolved in ethyl acetate:*n*-butanol:ethanol, loaded into a glass syringe (Hamilton Company, Reno, NV), and driven through the outer layer of the coaxial needle by a syringe pump (KD Scientific, KDS100). The aqueous solution containing murabutide, OVA, or FITC-BSA (fluorescein isothiocyanate conjugated to bovine serum albumin) (1% w/w of Ace-DEX) was loaded into a 0.5 mL glass syringe and pumped through the inner needle of the coaxial system. The organic and aqueous phases come into contact at the Taylor cone, which formed at the needle tip due to the high voltage applied between the needle (+2.5 kV) and the stainless steel collection plate (around -8 kV), located 10 cm below the needle tip. MPs were collected after the Taylor cone stabilized. The MP film was removed from the plate using a plastic putty scraper, lyophilized, and stored at -20 °C. Empty Ace-DEX MPs (EMPs) were prepared following the same protocol in the absence of murabutide or OVA. MP yield of the electrospray process was around 80%. Any loss was mostly due to inability to harvest all MPs from the collection plate or instability of the Taylor cone.

## 2.5. Encapsulation efficiency of murabutide and OVA

Encapsulated murabutide or OVA was quantified using a fluorescamine assay based on a modified protocol by Broaders et al. [29, 50]. MPs were prepared in triplicate, resuspended at 1 mg/mL in 0.3 M sodium acetate buffer (pH 5.0) with 1% sodium dodecyl sulfate, and incubated at 95 °C with gentle agitation for 20 min or until complete degradation. Samples (150 µL) were loaded onto a solvent-resistant 96-well plate together with a calibration curve containing free murabutide or OVA (0.313 – 20 µg/mL) and EMPs for background signals.

Fluorescamine (50  $\mu$ L, 3 mg/mL in dimethyl sulfoxide) was added to the wells before fluorescence signals (excitation 390, emission 460 nm) were measured using a SpectraMax M2 microplate reader (Molecular Devices, Sunnyvale, CA).

## 2.6 Encapsulation efficiency of FITC-BSA

FITC-BSA encapsulated Ace-DEX MPs were dissolved in ethanol at 1 mg/mL in triplicate and measured for fluorescence intensity (excitation 495 nm, emission 520 nm) using a microplate reader. Sample signals were compared to a standard curve of soluble FITC-BSA prepared following the same method to calculate encapsulation efficiency.

## 2.7. Physical characterization of Ace-DEX MPs

Size, morphology, and endotoxin level of Ace-DEX MPs were analyzed following a previously described protocol [49]. Briefly, MP size (Mean Diameter by Number) was measured by dynamic light scattering (DLS) using a Brookhaven NanoBrook 90Plus Zeta Particle Size Analyzer (Holtville, NY). DLS was used as opposed to laser diffraction in order to conserve samples. Size and morphology were visualized via scanning electron microscopy (SEM) using Hitachi s-4300 Cold Field Emission. The samples were assayed using Pierce LAL Chromogenic Endotoxin Quantitation Kit (Thermo Scientific, Waltham, MA) to confirm the absence of endotoxin.

## 2.8. Degradation analysis of Ace-DEX MPs

Empty Ace-DEX MPs of varying CAC (20%, 40%, or 60%) were resuspended in PBS (pH 7.4) or 1 M sodium phosphate buffer (pH 6.5) in triplicates (1.5 mg/mL) on a shaker plate at 37 °C to determine their degradation kinetics. PBS (pH 7.4) was selected to resemble neutral physiological environment (e.g. extracellular fluid), while the pH 6.5 buffer provides an environment that resembles the acidic condition observed within lysosomes of phagocytic cells [51]. The solution was vortexed at hour 0, 0.5, 2, 4, 8, 24, 48, 72, 168, and 336 to measure its absorbance at 600 nm via a SpectraMax M2 microplate reader (Molecular Devices, Sunnyvale, CA). We generated MPs' degradation profile by normalizing their absorbance levels at different time points to that at hour 0. The percent degradation of each sample is equal to the difference between its absorbance reading and that at hour 0 divided by the absorbance reading at hour 0, with the degradation half-life being the time it took for 50% of the MPs to be degraded.

## 2.9. Release kinetics of Ace-DEX MPs

Bovine serum albumin (BSA) was used as a model protein for OVA to examine the release kinetics of Ace-DEX MPs of different CAC. BSA-loaded MPs were fabricated via electrospray based on the same protocol described above. BSA-encapsulated MPs with 20%, 40%, or 60% CAC were incubated in PBS (pH = 7.4) or 1 M sodium phosphate buffer (pH 6.5) in triplicates (5 mg/mL) on a shaker plate at 37 °C. At 1, 5, 23, 30, 48, 72, and 192 hours, the solution was vortexed to collect an aliquot (170  $\mu$ L), which was centrifuged at 14,800 rpm for 15 min. Supernatant (150  $\mu$ L) was combined with ethanol (30  $\mu$ L) and stored at -20 °C. A sample (150  $\mu$ L) was removed from the vortexed solution at hour 192 and mixed with ethanol (30  $\mu$ L) to degrade any remaining MP, representing the total amount of



BSA (100% released). The amount of BSA was quantified using fluorescamine as described above, and the percent released was determined relative to the fluorescence signal of the respective MP set after complete degradation at the last time point.

### 2.10. In vitro cell viability analysis

Metabolic activity of JAWSII dendritic cells was analyzed using a 3-(4,5-dimethylthiazol-2-yl)-2,5-diphenyltetrazolium bromide (MTT) assay after co-culture with free or encapsulated-murabutide (3.2 – 400 ng/mL). Cells were seeded overnight in a 96-well plate at  $4 \times 10^4$  cells per well before incubation with different treatment groups for 24 or 48 hours. Murabutide-loaded Ace-DEX MPs (20%, 40%, or 60% CAC) were resuspended in culture media. Empty Ace-DEX (40%) MPs (EMPs) were tested at the same concentration (0.043 mg/mL) as that of MPs required to achieve the highest murabutide dose. Cells treated with media-only or with lipopolysaccharide (LPS, 100 ng/mL) were included as controls. MTT assay was performed post 24/48-hour incubation based on an established protocol [49]. Metabolic activity of bone marrow derived dendritic cells (BMDCs) was also analyzed post MP treatment in order to further assess cytotoxicity. BMDCs were prepared and cultured following a previously published protocol [52]. Cells were plated and treated as described above and incubated for 48 hours before MTT assay was performed. These experiments were repeated three times with three cell passages for consistency.

### 2.11. Intracellular trafficking of Ace-DEX MPs via confocal laser scanning microscopy analyses

BMDCs ( $2 \times 10^5$  cells per well) were plated within poly-d-lysine pre-coated coverslip chamber slides overnight before incubated with soluble or encapsulated FITC-BSA (1  $\mu$ g) or EMPs for 8 hours. Cells were washed three times with serum-free media, and cultured for another 1, 2, or 3 days before incubated with LysoTracker Red (500 nM, Molecular Probes) for 30 min at 37 °C. Cells were then washed three more times prior to imaging. The cohort incubated with soluble FITC-BSA was imaged directly after the 8-hour protein incubation without the 1, 2, or 3 day culture period. Live cell imaging was performed using laser scanning confocal microscopy (LSM710, Zeiss, 63x oil immersion objective), and the lysosomes appeared red in color were visualized under RITC (excitation 577 nm, emission 590 nm). Z-stack images (0.8  $\mu$ m) were obtained with laser intensity and other parameters kept consistent across all treatment conditions. Differential interference contrast (DIC) confocal images were collected simultaneously with transmitted light (excitation 488 nm). Sequential acquisition was used to avoid bleed-through between the two fluorescent channels. The extent of co-localization between FITC-BSA (green) and lysosomal compartments (LysoTracker Red) was quantified using the Jacop plug-in for Image J with background signals corrected [53]. The specific algorithm used was based on the Mander's overlap coefficient, which ranges from 0 to 1, with the former corresponding to non-overlapping green and red pixels and the latter reflecting 100% co-localization.

### 2.12. In vitro bioactivity of murabutide-loaded Ace-DEX MPs

Bioactivity of free or encapsulated murabutide on JAWSII dendritic cells was evaluated at various concentrations based on the production of inflammatory cytokines. Cells were seeded overnight in a 96-well plate at  $4 \times 10^4$  cells per well before incubation for 24 hours

with free murabutide, murabutide-loaded Ace-DEX (20%, 40%, or 60% CAC) MPs, EMPs (40% CAC), media-only, or LPS (100 ng/mL). The amount of MPs was adjusted based on encapsulation efficiencies to achieve the same murabutide dose across the groups. EMPs were tested at the same level as that of the highest particle dose required to achieve the same murabutide concentration. Culture media was collected 24 hours after incubation and transferred to a 96-well V-bottom plate to pellet residual cells and particles via centrifugation at 4200 rpm for 10 min at room temperature. Expression levels of interleukin (IL)-6 and tumor necrosis factor (TNF)- $\alpha$  in the supernatant were measured by enzyme-linked immunosorbent assay (ELISA) per manufacturer's instructions (Fisher Scientific, Hampton, NH). Three independent repeats using three cell passages were performed for consistency.

### 2.13. In vivo vaccination and antibody titer analysis

Female, 6–8 week old, C57BL/6 mice (n=8; Charles River Laboratories, Wilmington, MA) were immunized on Day 0 and 21 under an IACUC (Institutional Animal Care and Use Committee)-approved protocol with different treatment groups. To examine tunable adjuvant delivery, treatments included murabutide-loaded Ace-DEX MPs of various CAC (20%, 40%, or 60%) with soluble ovalbumin (solOVA), soluble murabutide (solMB) with EMPs (40%) with solOVA, Alhydrogel (alum; 250  $\mu$ g) with solOVA, solOVA alone, and PBS (Table 1). To examine tunable antigen delivery, a different mice cohort were vaccinated with OVA-encapsulated Ace-DEX MPs of various CAC (20%, 40%, or 60%) given with or without MPL, soluble OVA (solOVA) with MPL (10  $\mu$ g), solOVA with Alhydrogel (alum; 250  $\mu$ g), solOVA with EMPs (40%), solOVA alone, and PBS (Table 2). The amount of MPs was adjusted to deliver the same murabutide (5  $\mu$ g per mouse per injection) or OVA dose (10  $\mu$ g per mouse per injection). SolOVA was given at a constant level (10  $\mu$ g) across the groups. Immediately prior to administration, Ace-DEX MPs were resuspended in sterile PBS with vortex and bath sonication to aid the suspension. All treatments were delivered by subcutaneous injection (200  $\mu$ L) to the mouse flank. MPs were administered within 1 month after manufacturing.

Blood was collected via submandibular bleeding on Day -7, 14, 28, and 42 into BioOne MiniCollect Capillary Blood Collection System Tubes (Fisher Scientific, Hampton, NH). Sera samples were centrifuged at 6500 rpm for 10 min at 4 °C. Supernatant was collected, and OVA-specific serum antibody (IgG, IgG1, and IgG2b) concentrations were determined by ELISA following manufacturer's instructions (Chondrex, Redmond, WA). Antibody levels (ng/mL) were analyzed against a standard curve and log-transformed (base 10).

### 2.14. Ex vivo antigen recall cytokine analysis

Animals (n=4) from different treatment groups were euthanized on Day 28 with splenocytes harvested for cytokine analysis. Splenocytes were cultured in a 96-well plate at a density of  $1 \times 10^6$  cells per well (200  $\mu$ L) in Roswell Park Memorial Institute medium 1640 (Fischer Scientific, Pittsburgh, PA) with 10% fetal bovine serum (Hyclone, Pittsburgh, PA) and 1% penicillin-streptomycin (Fischer Scientific, Pittsburgh, PA) at 37 °C with 5% CO<sub>2</sub> and 100% relative humidity. Cells were stimulated with OVA protein (10  $\mu$ g/mL) for 24 hours before supernatants were collected and analyzed for interferon (IFN)-gamma ( $\gamma$ ), interleukin



(IL)-2, tumor necrosis factor (TNF)-alpha ( $\alpha$ ), and IL-6 production via ELISA per manufacturer's protocol (eBioscience, San Diego, CA). Background levels for unstimulated cells were subtracted from all groups to calculate cytokine concentrations.

A separate population of harvested splenocytes was stimulated with OVA<sub>257-264</sub> (SIINFEKL; 10  $\mu$ g/mL; AnaSpec, Fremont, CA) to perform the enzyme-linked immunosorbent spot (ELISpot) assay. In accordance with the manufacturer's protocol (eBioscience, San Diego, CA), cells were cultured in a pre-coated 96-well plate at a density of  $1 \times 10^6$  cells per well (200  $\mu$ L). After 24-hour incubation, the frequencies of IFN- $\gamma$  and IL-2 producing cells were determined, and background measurements for unstimulated cells were subtracted from all groups.

### 3. Results and Discussion

#### 3.1. Characterization of electro spray Ace-DEX MPs

Encapsulation efficiency and final weight loading of murabutide- or OVA-loaded Ace-DEX MPs can be found in Table 3. The high encapsulation efficiencies agreed with previously reported values for coaxial electro spray MPs and can be attributed to the electro spray fabrication technique [8, 54]. Due to the absence of a hardening process in an aqueous environment, which is commonly required for emulsion particle fabrication, electro spray allows for high encapsulation efficiencies of therapeutic cargos. Although murabutide has been analyzed in multiple pre-clinical and clinical studies, only the soluble molecule was used, causing the need for high doses and repeated administration in part due to the limited permeability of the charged murabutide molecule to the Nod2 receptor that resides in the cytosol [55-57]. In order to encapsulate murabutide to improve intracellular delivery, we initially attempted a double emulsion formulation (w/o/w), which resulted in negligible molecule loading (data not shown) possibly due to murabutide's positive charge and hydrophilicity. Thus, successful encapsulation using electro spray demonstrates advantages of the electro spray platform and contributes to the novelty of this study. Researchers have explored alternative strategies to deliver murabutide by encapsulating its hydrophobic derivatives (e.g. acyl murabutide) via nanoprecipitation [58, 59]. This approach may lead to increased risk of adverse side effects and higher manufacturing cost, compared to electro spray where no chemical modification is required. Besides high loading efficiencies, electro spray also allows for the encapsulation of sensitive cargos, such as protein/peptide antigens, that may be damaged when exposed to harsh solvents and large shear forces during emulsion particle fabrication [8, 54]. Therefore, efficient adjuvant (murabutide) and antigen (OVA) encapsulation can increase delivery efficiency, promote therapeutic efficacy, limit adverse side effects, achieve dose sparing, and enable intracellular antigen delivery and cross-presentation after MP passive targeting to APCs.

Empty, murabutide-, and OVA-loaded MPs prepared from Ace-DEX of varying CAC (20%, 40%, or 60%) shared similar sizes and morphologies (Table 3 and Figure 1). MP size and morphology were independent of adjuvant or antigen loading or Ace-DEX CAC, and were both in agreement with previous findings by Gallovic et al. [8]. Average diameter measured by DLS was smaller than that observed in SEM images. This was due to number-weighted average measured by DLS weights each counted particle equally, and smaller particles,

which may be overshadowed in the SEM images, skewed the average diameter to the much smaller range. Given the major population of MPs are larger (around 1  $\mu\text{m}$ ) as observed in the SEM, they are properly sized for passive targeting to APCs [60]. All MP formulations were clear from endotoxin based on the FDA's guideline for sterile water [61].

Degradation profiles of Ace-DEX MPs of varying CAC are shown in Figure 2. Under both neutral (pH 7.4) and acidic (pH 6.5) conditions, MP degradation half-life related directly to Ace-DEX CAC, with 20% MPs hydrolyzed the fastest compared with 40% or 60% MPs. Hydrolysis occurred more rapidly within the acidic environment, which underlines the acid-sensitive nature of Ace-DEX MPs. Half-lives of 40% and 60% MPs at pH 7.4 are reported as greater than 336 hours since less than 50% of the MPs were degraded at this final time point. This trend between degradation half-life and MP CAC agreed with previous findings for emulsion Ace-DEX MPs [49], and can be attributed to higher percentage of the hydrolytically stable cyclic acetals versus acyclic acetals in MPs of higher CAC. It was observed that electrospray MPs exhibited longer half-lives than their emulsion counterparts of the same CAC, which can be explained by different pH conditions (5.0 vs. 6.5) and smaller surface area to volume ratio of electrospray MPs.

Release kinetics of Ace-DEX MPs of different CAC were characterized using BSA as a model protein for OVA. Limited publications are available that show OVA release from particles due to its instability at low pH levels. Radiolabeled or fluorescently labeled OVA was used by Osswald et al. or Gallovic et al., respectively in order to obtain strong, reproducible signals [50, 62]. We therefore, used BSA as a substitute, due to its similar molecular weight and isoelectric point (pI) (67.0 kDa; pI 4.7) to OVA (43.0 kDa; pI 4.5) [63, 64]. Faster release of encapsulated BSA was observed from MPs of lower CAC at both pH 7.4 and 6.5 (Supplementary Figure S1). At pH 7.4, 91.8% BSA was released by 48 hours for 20% MPs, which was substantially higher compared to 17.2% for 40% MPs or 5.65% for 60% MPs. Because MPs of lower CAC degrade more rapidly, a larger amount of the cargo was released into the supernatant. Using Ace-DEX of different CAC, burst and sustained release of encapsulated proteins can be achieved using the same delivery platform, which makes Ace-DEX an ideal carrier for vaccine applications where immune activation operates following precise temporal control. Under acidic environment (pH 6.5), the correlation between protein release and polymer CAC held true, with higher rates for all MP sets compared to their counterparts under the neutral pH. The higher release rate was due to Ace-DEX's acid-sensitive hydrolysis, which promotes antigen processing through cross-presentation, making Ace-DEX advantageous over other delivery vehicles [29]. Similar release profiles were observed by Gallovic et al. for Texas Red-labeled OVA encapsulated within emulsion MPs made from acetalated inulin (Ace-IN). Approximately 20% and 55% of the OVA was released from Ace-IN (26.7% CAC) MPs by 168 hours at pH 7.4 and 6.5, respectively, which largely agrees with our findings [50].

To further examine cargo release within cellular compartments, intracellular trafficking of FITC-BSA encapsulated MPs was analyzed. Both fast- and slow-degradation MPs (20% and 60% CAC, respectively) showed significant levels of co-localization between FITC-BSA and lysosomes, suggesting efficient MP uptake by BMDCs (Figure 3). Co-localization levels decreased overtime for both 20% and 60% MP groups with gradual increase in % non-

localized ((1-Mander's overlap coefficient)  $\times$  100%), which is likely due to MP degradation and suggests cargo release into the cytosol. Lower levels of MP/lysosome co-localization and greater values of % non-localized were observed for MPs of 20% CAC. This can likely be attributed to their faster degradation (Figure 2) and more rapid cargo release (Supplementary Figure S1). Tunable intracellular release enabled by controlled degradation of Ace-DEX MPs demonstrates advantage of our platform, which can be beneficial for vaccine delivery. It is also important to note both MP sets yielded higher levels of fluorescence signals compared to the soluble FITC-BSA control, which suggested enhanced delivery efficiency via MP encapsulation. The absence of fluorescence intensity when BMDCs were incubated with EMPs indicates little background signal from the Ace-DEX vehicle (Supplementary Figure S2).

### 3.2. In vitro bioactivity of murabutide-loaded Ace-DEX MPs

Bioactivity of encapsulated murabutide was first compared to its soluble form *in vitro* with JAWSII dendritic cells at various concentrations for IL-6 and TNF- $\alpha$  expression. Although both free and encapsulated murabutide exhibited dose-dependent responses, murabutide-loaded Ace-DEX (40%) MPs resulted in significantly higher levels of IL-6 expression than that of the soluble adjuvant at all concentrations tested (0.625 – 10  $\mu$ g/mL) (Supplementary Figure S3). When encapsulated within Ace-DEX MPs of varying CAC (20%, 40%, or 60%) and tested at lower concentrations (3.2 – 400 ng/mL), murabutide again outperformed its soluble form for IL-6 and TNF- $\alpha$  production (Figure 4B and 4C). This dose sparing agreed with previous findings of increased adjuvant activity via particulate encapsulation [65, 66], and can be explained by enhanced cellular uptake and intracellular access of the adjuvant. After being phagocytosed by APCs, acid-labile Ace-DEX MPs degrade rapidly within acidic phagosomes and release encapsulated murabutide, which can escape and bind to its cytosolic receptor Nod2. Despite being studied in multiple clinical trials, murabutide often requires repeated, high-dose administration in part due to limited cell permeability of the charged molecule [57, 67]. In particular, subcutaneous injections (7 mg) for 5 consecutive days/week for 6 weeks were required for Bahr et al. to test murabutide's clinical effects on HIV-1 patients [57]. Therefore, enhanced adjuvant delivery via MP encapsulation illustrates promising dose sparing and highlights the potential of the Ace-DEX delivery platform.

When murabutide was encapsulated within Ace-DEX MPs of different CAC, the adjuvant showed similar levels of cytokine production (Figure 4B and 4C), which may result from compound saturation. Comparable degrees of cellular metabolic activity (around 100%) were observed based on the MTT assay for immortal and primary dendritic cells cultured with soluble or encapsulated murabutide, or with empty MPs (Figure 4A and Supplementary Figure S4), suggesting limited cytotoxicity. It agreed with previous findings [49, 68], and represents another advantage of Ace-DEX MPs over MPs fabricated from other acid-sensitive polymers, such as PBAEs, which caused 60% reduction in cellular metabolic activity at 0.1 mg/mL [26, 40].

### 3.3. In vivo vaccination and antibody titer analysis

Magnitude and kinetics of humoral and cellular immune responses were determined through a 6-week murine study using murabutide or OVA encapsulated within Ace-DEX MPs of

various CAC. To examine the effect of controlled adjuvant delivery, we vaccinated C57BL/6 mice with soluble OVA and murabutide-encapsulated in Ace-DEX (20%, 40%, or 60%) MPs on Day 0 and 21 (Table 1). OVA-specific humoral responses (IgG, IgG1, and IgG2b) were measured for sera collected Day -7, 14, 28, and 42 post prime immunization. On Day 14 and 28, an inverse relationship between antibody titers and polymer CAC was observed, with higher antibody levels associated with MPs of lower CAC (Figure 5 and Supplementary Table S1). This correlation was not as obvious when MPs were tested *in vitro* (Figure 4), possibly due to the complexity of a living organism compared to cultured cells, making it difficult to translate *in vitro* results to *in vivo* settings. The inverse relationship between antibody titers and polymer CAC changed at later time points (Day 42) (Figure 5 and Supplementary Table S1). While Ace-DEX (40%) MPs continued to generate higher IgG and IgG2b levels than 60% MPs, 20% MPs resulted in the lowest level of antibody response. This drop in antibody titers might be explained by rapid degradation and short half-life of 20% MPs. Because 20% MPs hydrolyze more rapidly, they offered lower levels of adjuvant exposure to APCs due to the fastest clearance, which may also be attributed to the lower antibody levels for 20% MPs on Day 42 compared to that on Day 28. Therefore, MPs of varying CAC elicited peak immunity at different time points, suggesting different MP sets could be selected to tune immune activation based on the disease of interest. Ace-DEX MPs of lower CAC (fast degrading) may be beneficial to fighting diseases requiring a rapid antibody response or for individuals who need protection quickly, such as anthrax [69], whereas MPs of higher CAC (slow degrading) may be advantageous for conditions that would benefit from a more sustained immune response, such as malaria where stronger efficacy was observed with longer prime-boost intervals due to the greater time needed for memory cell maturation [19]. As the Ace-DEX MP platform enabled controlled immune activation over a wide range of time frames, it serves as a promising candidate for tunable adjuvant delivery, contributing to improved efficacy and enhanced safety profiles of adjuvanted vaccines.

When comparing encapsulated to soluble murabutide, we found that the encapsulated adjuvant induced stronger humoral responses as measured by IgG, IgG1, and IgG2b titer levels, suggesting promoted adjuvant potency via particulate delivery, likely due to enhanced cellular uptake and boosted intracellular access. Moreover, encapsulated murabutide generated a more balanced Th1/Th2 response than that by the benchmark formulation, solOVA/alum (Figure 5). Strong IgG1 and weak IgG2b responses were observed for the solOVA/alum vaccination since alum is Th2-biased [70]. In comparison, murabutide MPs with solOVA exhibited a more balanced Th1/Th2 response with strong IgG1 and moderate IgG2b production, which is advantageous for fighting against cancer and intracellular infections [71]. Murabutide signaling through the NF- $\kappa$ B pathway via Nod2 receptor might have contributed to the enhanced Th1 response, which was further promoted by increased intracellular adjuvant delivery via MP encapsulation [45, 72, 73]. The balanced Th1/Th2 response might also result from free antigen getting adsorbed onto the MP surface, carried into APC through phagocytosis, and cross-presented at the major histocompatibility complex class I. This observation agreed with previous findings [8], and is important considering the essential role played by Th1 response in the clearance of intracellular

pathogens such as HIV that murabutide has shown effective against in multiple clinical trials [74–76].

After demonstrating the effect of varying MP CAC on adjuvant delivery and immune activation kinetics, we pursued the impact of controlled antigen delivery on immune responses by monitoring the magnitude and kinetics of humoral and cellular immunity of mice vaccinated with OVA-encapsulated MPs of various CAC, co-delivered with soluble MPL (Table 2). For animals receiving OVA-loaded MPs of lower CAC, higher antibody levels were generally observed, resulting from faster MP hydrolysis and more rapid antigen release (Figure 6 and Supplementary Table S1). This observed control over immune activation based on different antigen release kinetics is advantageous at promoting tailored immune responses for particular diseases of interest by tuning the peak and duration of protective immunity. While effector T cells require 1-hour antigen stimulation to become activated, longer antigenic signaling (from 20 hours up to 2–3 days) is needed by naive T cells before committed to proliferation [24]. Memory T cells, on the other hand, demand for booster stimulation for activation [77]. Prolonged or high dose stimulation can lead to cell death or immunotolerance, which lowers vaccine efficacy [78]. Since different disease treatment relies on activation of distinct cell populations: effector T cell proliferation is needed for quick protection, while memory T cells activation is required for sustained immunity, control over immune activation kinetics is important at optimizing protective immunity profiles for different diseases of interest. Therefore, Ace-DEX MPs that allow for tunable antigen release and controlled immune activation could greatly contribute to the development of safer and more effective vaccines [79]. Previous attempts for controlled antigen delivery often used mixed polymers that exhibit different release profiles and focused on *in vitro* characterization with limited results on *in vivo* efficacy testing [80–82]. Feng et al. reported control of antigen delivery using PLGA particles of different polymer composition: PLGA50/50 microspheres, PLGA75/25 microspheres, or a mixture of PLGA50/50, PLGA75/25, and PLGA50/50-COOH microspheres [82]. Although PLGA microspheres exhibited greater potency than the soluble antigen, no significant difference was observed in antibody production when antigen was delivered by different vehicles (PLGA50/50, PLGA75/25, or a mixture of microspheres), possibly due to slow hydrolysis and limited tunability in PLGA degradation. DeMuth et al. used silk/poly(acrylic acid) (PAA) composite microneedles for a combined bolus/sustained delivery, with the PAA bases rapidly releasing a vaccine bolus and the silk hydrogel providing a sustained release [83]. Despite promising results in promoting immune responses, this microneedle approach is limited to local inflammatory responses caused by skin-resident dendritic cells (e.g. Langerhan cells), and the use of mixed materials may also lead to complex manufacturing procedure and increased risk of adverse side effects. Wang et al. explored the use of different acid-labile poly(ortho ester) microsphere formulations for tunable DNA vaccine delivery [84]. They observed boosted immunogenicity over PLGA particles, which supports the advantages of acid-sensitive vehicles.

It is important to note that the inverse relationship between antibody response and Ace-DEX MP CAC held true across all time points for antigen (OVA) administration, which is different from that for adjuvant (murabutide) delivery where the trend reversed to a correlative relationship at the last time point. This discrepancy supports the need for distinct,

flexible control over adjuvant or antigen delivery as immune response kinetics differ after vaccination and may vary based on the disease of interest. Since adjuvant and antigen molecules undergo different activation and signaling pathways followed by various APC-T cell interactions, immune responses post adjuvant or antigen uptake follow distinct timelines. This makes Ace-DEX controlled delivery more advantageous by tuning temporal release of different vaccine elements separately to optimize immune response profiles based on the disease of interest. Previous observation by our lab and others support superior activity of single-encapsulated vaccine components within separate particulate formulations compared to co-encapsulated cargos within the same delivery vehicle. Gallovic et al. showed enhanced protection against lethal Anthrax challenge by co-delivery of separate Ace-DEX MPs containing either Anthrax antigen protective antigen (PA) or toll-like receptor 7/8 agonist resiquimod (R848), compared to MPs loaded with both PA and R848 [47]. Ilyinskii et al., among others, also demonstrated potentiated IgG titers with separate particle encapsulation compared to co-encapsulation [85–87]. The superior activity of separate versus co-encapsulation echoes the potential of differential immune response kinetics post adjuvant or antigen vaccination. This highlights the significant advantage of the Ace-DEX MP platform that enables controlled adjuvant or antigen delivery to distinctly tailor the release profiles of different vaccine elements for controlled immune activation [47]. Although there is differing literature reporting similar or greater immunogenicity of co-encapsulated adjuvant or antigen [88, 89], most reports compared co-encapsulated formulations to one encapsulated component in combination with one soluble component, with limited data available where a side-by-side comparison to separately encapsulated antigen and adjuvant was included. Moreover, none of these reports conducted a challenge experiment, except for Gallovic et al. who demonstrated enhanced protection of separately encapsulated MPs during a lethal Anthrax challenge - highlighting the superior protective efficacy of separate adjuvant or antigen MPs. Since Ace-DEX MPs of varying CAC could be selected to control immune activation over a wide range of time frames, it represents a promising platform to finely tune the level and duration of inflammatory signals for controlled adjuvant or antigen delivery. Antigen encapsulation within Ace-DEX MPs also boosted its humoral immunogenicity as shown by higher antibody levels of encapsulated OVA (OVA MPs without MPL) compared to that of animals receiving soluble OVA alone or with EMPs (Figure 6). Encapsulated OVA generated higher IgG2b production than the alum-adsorbed OVA, which suggested enhanced Th1 response, supporting previous findings of promoted antigen cross-presentation by MP encapsulation and underlining advantages of the Ace-DEX delivery platform over the benchmark solOVA/alum formulation due to the more balanced Th1/Th2 response [29].

### 3.4. Ex vivo antigen recall analysis

We characterized cytokine expression profiles of antigen re-stimulated splenocytes harvested from vaccinated mice on Day 28, to analyze the effect of tunable adjuvant or antigen delivery on cellular immune responses.

To study controlled adjuvant delivery, animals were immunized with murabutide-encapsulated MPs of varying CAC. Higher inflammatory cytokine production (IFN- $\gamma$ , IL-2, and TNF- $\alpha$ ) was generally observed for splenocytes harvested from mice that received Ace-



DEX MPs of lower CAC (20%), compared to those of 40% or 60% CAC (Figure 7A–C). This inverse relationship agreed with the antibody titer profile on Day 28. MPs with lower CAC degraded faster, thereby potentially releasing a larger amount of adjuvant, leading to a stronger immune response and higher cytokine production. This controlled cellular activation supplemented the tunable humoral response, and are important for disease treatment requiring distinct immune responses. Furthermore, encapsulated murabutide induced higher cytokine expression than that of the soluble adjuvant or the benchmark formulation (solOVA/alum), which echoes the greater antibody titer response observed for the encapsulated adjuvant, illustrating potent efficacy of the MP delivery platform.

Effects of tunable antigen delivery were analyzed and compared with those when delivering the adjuvant. For mice immunized with MPL-adjuvanted OVA-encapsulated MPs of varying CAC, there was higher cytokine production (IFN- $\gamma$ , IL-2, and TNF- $\alpha$ ) for MP vaccines of lower CAC (Figure 7D–F). This trend agrees with that of the antibody production, and also resembles that observed for adjuvant delivery. Similar to antibody production, enhanced Th1 cytokine responses to OVA antigen were observed through MP encapsulation, as demonstrated by significantly higher IL-2 levels, and greater production of IFN- $\gamma$  and TNF- $\alpha$  on average. MP-encapsulated OVA also generated more potent cytokine responses than those by the benchmark formulation (solOVA/alum), which together with the higher IgG2b levels, suggested potent cellular immune activation.

Frequencies of antigen-specific IFN- $\gamma$ - and IL-2-producing splenocytes were also examined for mice receiving encapsulated murabutide or OVA to study controlled adjuvant or antigen delivery. The number of IFN- $\gamma$ - or IL-2-producing cells generally related inversely to polymer CAC for both murabutide (Figure 8A, 8B and Supplementary Table S2) or OVA/MPL-immunized (Figure 8C, 8D and Supplementary Table S3) mice. This inverse relationship agrees with the observed trend for antibody or cytokine production, highlighting controlled immune modulation at both humoral and cellular levels by the Ace-DEX MP system. Encapsulated murabutide outperformed solOVA/alum at promoting the number of cytokine-producing cells, which together with the promoted cytokine production indicates a more balanced Th1/Th2 immune response, in support of the high IgG2b antibody titer. Overall, the enhanced adjuvant activity, promoted antigen immunogenicity, balanced immune response, and tunable humoral and cellular activation demonstrate advantages of the Ace-DEX MP delivery platform over existing systems and suggest its contribution to the development of safer and more efficacious subunit vaccines.

## 4. Conclusions

In this study we analyzed immune response kinetics to adjuvant or antigen delivery via Ace-DEX MPs of varying CAC encapsulating either adjuvant or antigen. Considering the significant impact of the kinetics and duration of protective immunity for different diseases of interest, precise control over adjuvant or antigen release and immune activation could substantially enhance the safety and effectiveness of subunit vaccines. When tested for adjuvant delivery, MPs of lower CAC (20%) induced stronger antibody response and cytokine expression at earlier time points, while MPs of 40% or 60% CAC elicited greater antibody titers at the last time point. When tested for antigen delivery, MPs of lower CAC

induced more potent humoral and cellular responses throughout the entire experimental period. This differential response supports the distinct kinetics for adjuvant or antigen delivery, indicates the importance of separate, flexible control over vaccine element administration, and suggests its potential contribution to optimal immunogenicity. Facile tunability enabled by the Ace-DEX delivery platform allows for distinct control over adjuvant or antigen delivery, and both burst and sustained vaccine activity using the same polymeric platform, making Ace-DEX MPs a promising candidate for controlled vaccine formulations. To the best of our knowledge, we are the first to demonstrate controlled immune activation following *in vivo* vaccination using a single polymeric delivery platform. Future work exploring the kinetics of immune activation, pathway signaling, and antigen-APC interaction will improve our understanding for adjuvant or antigen delivery, further demonstrate the novelty of our tunable delivery platform, and promote its contribution to the development of safer and more effective vaccines.

## Supplementary Material

Refer to Web version on PubMed Central for supplementary material.

## Acknowledgments

This work was supported by Internal Funds of the University of North Carolina at Chapel Hill and the National Institutes of Health U19 AI109784. The authors are appreciative of the help from UNC Chapel Hill Analytical and Nanofabrication Laboratory in acquiring SEM images. We would also like to thank the UNC CFAR Virology, Immunology, and Microbiology Core for their ELISpot reader.

## References

1. Akagi T, Baba M, Akashi M. Biodegradable Nanoparticles as Vaccine Adjuvants and Delivery Systems: Regulation of Immune Responses by Nanoparticle-Based Vaccine. *Polymers in Nanomedicine*. 2011;31–64.
2. O'Hagan DT, Rappuoli R. Novel approaches to vaccine delivery. *Pharm Res*. 2004; 21(9):1519–30. [PubMed: 15497674]
3. Glenney AT, et al. XXIII: the Antigenic Value of Toxoid Precipitated by Potassium Alum. *J Pathol Bacteriol*. 1926; 29:2.
4. Banzhoff A, et al. MF59-adjuvanted vaccines for seasonal and pandemic influenza prophylaxis. *Influenza Other Respir Viruses*. 2008; 2(6):243–9. [PubMed: 19453401]
5. Tagliabue A, Rappuoli R. Vaccine adjuvants: the dream becomes real. *Hum Vaccin*. 2008; 4(5):347–9. [PubMed: 18682690]
6. Doherty PC, et al. Influenza and the challenge for immunology. *Nat Immunol*. 2006; 7(5):449–55. [PubMed: 16622432]
7. Baylor NW, Egan W, Richman P. Aluminum salts in vaccines--US perspective. *Vaccine*. 2002; 20(Suppl 3):S18–23. [PubMed: 12184360]
8. Gallovic MD, et al. Acetalated Dextran Microparticulate Vaccine Formulated via Coaxial Electrospray Preserves Toxin Neutralization and Enhances Murine Survival Following Inhalational Bacillus Anthracis Exposure. *Adv Healthc Mater*. 2016; 5(20):2617–2627. [PubMed: 27594343]
9. Joshi VB, Geary SM, Salem AK. Biodegradable particles as vaccine antigen delivery systems for stimulating cellular immune responses. *Hum Vaccin Immunother*. 2013; 9(12):2584–90. [PubMed: 23978910]
10. Zhang Y, Chan HF, Leong KW. Advanced materials and processing for drug delivery: the past and the future. *Adv Drug Deliv Rev*. 2013; 65(1):104–20. [PubMed: 23088863]

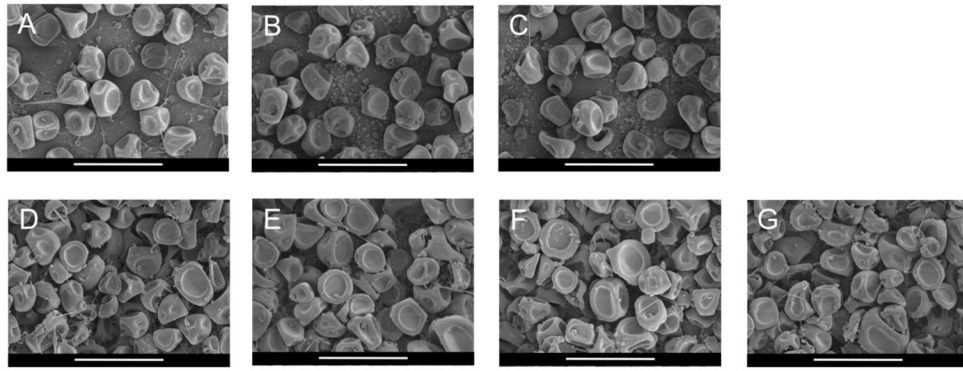
11. Manolova V, et al. Nanoparticles target distinct dendritic cell populations according to their size. *Eur J Immunol*. 2008; 38(5):1404–13. [PubMed: 18389478]
12. Coffman RL, Sher A, Seder RA. Vaccine adjuvants: putting innate immunity to work. *Immunity*. 2010; 33(4):492–503. [PubMed: 21029960]
13. Makadia HK, Siegel SJ. Poly Lactic-co-Glycolic Acid (PLGA) as Biodegradable Controlled Drug Delivery Carrier. *Polymers (Basel)*. 2011; 3(3):1377–1397. [PubMed: 22577513]
14. Fu K, et al. Visual evidence of acidic environment within degrading poly(lactic-co-glycolic acid) (PLGA) microspheres. *Pharm Res*. 2000; 17(1):100–6. [PubMed: 10714616]
15. Tobio M, Jose Alonso M. Study of the Inactivation Process of the Tetanus Toxoid in Contact with Poly(lactic/glycolic acid) Degrading Microspheres. *STPPharma Sciences*. 1998; 8(5):8.
16. Liu Y, et al. The microclimate pH in poly(D,L-lactide-co-hydroxymethyl glycolide) microspheres during biodegradation. *Biomaterials*. 2012; 33(30):7584–93. [PubMed: 22819499]
17. Zhu G, Mallery SR, Schwendeman SP. Stabilization of proteins encapsulated in injectable poly (lactide- co-glycolide). *Nat Biotechnol*. 2000; 18(1):52–7. [PubMed: 10625391]
18. Haining WN, et al. pH-triggered microparticles for peptide vaccination. *J Immunol*. 2004; 173(4): 2578–85. [PubMed: 15294974]
19. Brice GT, et al. Extended immunization intervals enhance the immunogenicity and protective efficacy of plasmid DNA vaccines. *Microbes Infect*. 2007; 9(12–13):1439–46. [PubMed: 17913540]
20. Ledgerwood JE, et al. Prime-boost interval matters: a randomized phase 1 study to identify the minimum interval necessary to observe the H5 DNA influenza vaccine priming effect. *J Infect Dis*. 2013; 208(3):418–22. [PubMed: 23633407]
21. Zinkernagel RM, et al. Antigen localisation regulates immune responses in a dose- and time-dependent fashion: a geographical view of immune reactivity. *Immunol Rev*. 1997; 156:199–209. [PubMed: 9176709]
22. Zinkernagel RM. Localization dose and time of antigens determine immune reactivity. *Semin Immunol*. 2000; 12(3):163–71. discussion 257–344. [PubMed: 10910735]
23. Wang Q, et al. Time course study of the antigen-specific immune response to a PLGA microparticle vaccine formulation. *Biomaterials*. 2014; 35(29):8385–93. [PubMed: 24986256]
24. Iezzi G, Karjalainen K, Lanzavecchia A. The duration of antigenic stimulation determines the fate of naive and effector T cells. *Immunity*. 1998; 8(1):89–95. [PubMed: 9462514]
25. Obst R. The Timing of T Cell Priming and Cycling. *Front Immunol*. 2015; 6:563. [PubMed: 26594213]
26. Kauffman KJ, et al. Synthesis and characterization of acetalated dextran polymer and microparticles with ethanol as a degradation product. *ACS Appl Mater Interfaces*. 2012; 4(8): 4149–55. [PubMed: 22833690]
27. Kanthamneni N, et al. Enhanced stability of horseradish peroxidase encapsulated in acetalated dextran microparticles stored outside cold chain conditions. *Int J Pharm*. 2012; 431(1–2):101–10. [PubMed: 22548844]
28. Peine KJ, et al. Efficient delivery of the toll-like receptor agonists polyinosinic:polycytidylic acid and CpG to macrophages by acetalated dextran microparticles. *Mol Pharm*. 2013; 10(8):2849–57. [PubMed: 23768126]
29. Broaders KE, et al. Acetalated dextran is a chemically and biologically tunable material for particulate immunotherapy. *Proc Natl Acad Sci U S A*. 2009; 106(14):5497–502. [PubMed: 19321415]
30. Chen N, et al. Degradation of acetalated dextran can be broadly tuned based on cyclic acetal coverage and molecular weight. *Int J Pharm*. 2016; 512(1):147–157. [PubMed: 27543351]
31. Griffin JF, Mackintosh CG, Rodgers CR. Factors influencing the protective efficacy of a BCG homologous prime-boost vaccination regime against tuberculosis. *Vaccine*. 2006; 24(6):835–45. [PubMed: 16098638]
32. Suarez S, et al. Tunable protein release from acetalated dextran microparticles: a platform for delivery of protein therapeutics to the heart post-MI. *Biomacromolecules*. 2013; 14(11):3927–35. [PubMed: 24053580]

33. Suarez S, et al. Degradable Acetalated Dextran Microparticles for Tunable Release of an Engineered Hepatocyte Growth Factor Fragment. *Biomater Sci.* 2016; 2(2):8.
34. Bachelder EM, et al. Acetal-derivatized dextran: an acid-responsive biodegradable material for therapeutic applications. *J Am Chem Soc.* 2008; 130(32):10494–5. [PubMed: 18630909]
35. Gupta P, et al. Degradation of poly(beta-amino ester) gels in alcohols through transesterification: method to conjugate drugs to polymer matrices. *Journal of Polymer Science: Polymer Chemistry.* 2017; 55(12):8.
36. Song C, et al. Oxidation-accelerated hydrolysis of the ortho ester-containing acid-labile polymers. *ACS Macro Letters.* 2013; 2(3):5. [PubMed: 23336091]
37. Yang SC, et al. Polyketal copolymers: a new acid-sensitive delivery vehicle for treating acute inflammatory diseases. *Bioconjug Chem.* 2008; 19(6):1164–9. [PubMed: 18500834]
38. Anderson JM, Rodriguez A, Chang DT. Foreign body reaction to biomaterials. *Semin Immunol.* 2008; 20(2):86–100. [PubMed: 18162407]
39. Little SR, et al. Poly-beta amino ester-containing microparticles enhance the activity of nonviral genetic vaccines. *Proc Natl Acad Sci U S A.* 2004; 101(26):9534–9. [PubMed: 15210954]
40. Little SR, et al. Formulation and characterization of poly (beta amino ester) microparticles for genetic vaccine delivery. *J Control Release.* 2005; 107(3):449–62. [PubMed: 16112767]
41. Ji R, et al. Shell-sheddable, pH-sensitive supramolecular nanoparticles based on ortho ester-modified cyclodextrin and adamantyl PEG. *Biomacromolecules.* 2014; 15(10):3531–9. [PubMed: 25144934]
42. Paramonov SE, et al. Fully acid-degradable biocompatible polyacetal microparticles for drug delivery. *Bioconjug Chem.* 2008; 19(4):911–9. [PubMed: 18373356]
43. Chedid LA, et al. Biological activity of a new synthetic muramyl peptide adjuvant devoid of pyrogenicity. *Infect Immun.* 1982; 35(2):417–24. [PubMed: 7035362]
44. Geddes K, Magalhaes JG, Girardin SE. Unleashing the therapeutic potential of NOD-like receptors. *Nat Rev Drug Discov.* 2009; 8(6):465–79. [PubMed: 19483708]
45. Jakopin Z. Murabutide revisited: a review of its pleiotropic biological effects. *Curr Med Chem.* 2013; 20(16):2068–79. [PubMed: 23531213]
46. Casella CR, Mitchell TC. Putting endotoxin to work for us: monophosphoryl lipid A as a safe and effective vaccine adjuvant. *Cell Mol Life Sci.* 2008; 65(20):3231–40. [PubMed: 18668203]
47. Gallovic MD, et al. Acetalated Dextran Microparticulate Vaccine Formulated via Coaxial Electrospray Preserves Toxin Neutralization and Enhances Murine Survival Following Inhalational Bacillus Anthracis Exposure. *Adv Healthc Mater.* 2016
48. Duong AD, et al. Electrospray Encapsulation of Toll-Like Receptor Agonist Resiquimod in Polymer Microparticles for the Treatment of Visceral Leishmaniasis. *Molecular Pharmaceutics.* 2013; 10(3):1045–1055. [PubMed: 23320733]
49. Chen N, et al. Degradation of acetalated dextran can be broadly tuned based on cyclic acetal coverage and molecular weight. *Int J Pharm.* 2016; 512(1):147–57. [PubMed: 27543351]
50. Gallovic MD, et al. Chemically modified inulin microparticles serving dual function as a protein antigen delivery vehicle and immunostimulatory adjuvant. *Biomater Sci.* 2016; 4(3):483–93. [PubMed: 26753184]
51. McNeil PL, et al. Acidification of phagosomes is initiated before lysosomal enzyme activity is detected. *J Cell Biol.* 1983; 97(3):692–702. [PubMed: 6885916]
52. Alpan O, et al. 'Educated' dendritic cells act as messengers from memory to naive T helper cells. *Nat Immunol.* 2004; 5(6):615–22. [PubMed: 15156140]
53. Bolte S, Cordeliers FP. A guided tour into subcellular colocalization analysis in light microscopy. *J Microsc.* 2006; 224(Pt 3):213–32. [PubMed: 17210054]
54. Xu Q, et al. Coaxial electrohydrodynamic atomization process for production of polymeric composite microspheres. *Chem Eng Sci.* 2013:104.
55. Feinen B, et al. Advax-adjuvanted recombinant protective antigen provides protection against inhalational anthrax that is further enhanced by addition of murabutide adjuvant. *Clin Vaccine Immunol.* 2014; 21(4):580–6. [PubMed: 24554695]

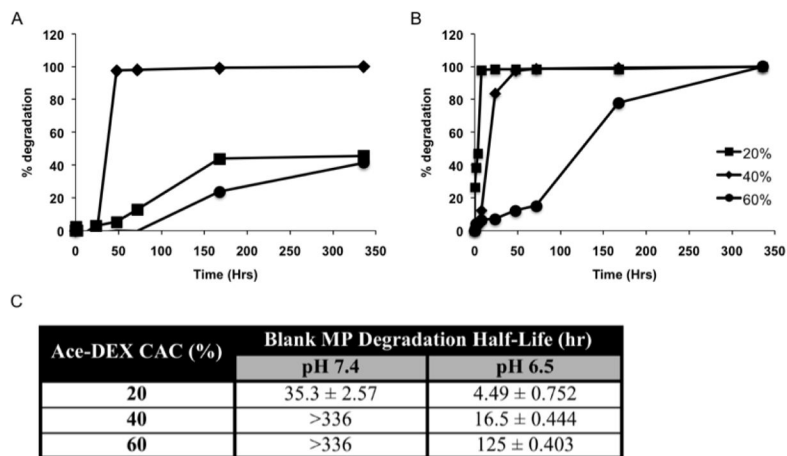
56. Jackson EM, Herbst-Kralovetz MM. Intranasal vaccination with murabutide enhances humoral and mucosal immune responses to a virus-like particle vaccine. *PLoS One*. 2012; 7(7):e41529. [PubMed: 22855691]
57. Bahr GM, et al. Clinical and immunological effects of a 6 week immunotherapy cycle with murabutide in HIV-1 patients with unsuccessful long-term antiretroviral treatment. *J Antimicrob Chemother*. 2003; 51(6):1377–88. [PubMed: 12716777]
58. Pavot V, et al. Encapsulation of Nod1 and Nod2 receptor ligands into poly(lactic acid) nanoparticles potentiates their immune properties. *J Control Release*. 2013; 167(1):60–7. [PubMed: 23352911]
59. Pavot V, et al. Directing vaccine immune responses to mucosa by nanosized particulate carriers encapsulating NOD ligands. *Biomaterials*. 2016; 75:327–39. [PubMed: 26539801]
60. Kohane DS. Microparticles and nanoparticles for drug delivery. *Biotechnol Bioeng*. 2007; 96(2): 203–9. [PubMed: 17191251]
61. Bacterial Endotoxins/Pyrogens. [cited 2017; <https://www.fda.gov/ICECI/Inspections/InspectionGuides/InspectionTechnicalGuides/ucm072918.htm>]
62. Osswald CR, Kang-Mieler JJ. Controlled and Extended Release of a Model Protein from a Microsphere-Hydrogel Drug Delivery System. *Ann Biomed Eng*. 2015; 43(11):2609–17. [PubMed: 25835212]
63. Ge S, et al. Bovine serum albumin adsorption onto immobilized organotrichlorosilane surface: influence of the phase separation on protein adsorption patterns. *J Biomater Sci Polym Ed*. 1998; 9(2):131–50. [PubMed: 9493841]
64. Israel OK. Adsorption of the proteins of white wine onto activated carbon, alumina and titanium dioxide. 2009
65. Tacken PJ, et al. Targeted delivery of TLR ligands to human and mouse dendritic cells strongly enhances adjuvanticity. *Blood*. 2011; 118(26):6836–44. [PubMed: 21967977]
66. Westwood A, et al. Immunological responses after immunisation of mice with microparticles containing antigen and single stranded RNA (polyuridylic acid). *Vaccine*. 2006; 24(11):1736–43. [PubMed: 16278038]
67. Amiel C, et al. Clinical tolerance and immunologic effects after single or repeated administrations of the synthetic immunomodulator murabutide in HIV-1-infected patients. *J Acquir Immune Defic Syndr*. 2002; 30(3):294–305. [PubMed: 12131566]
68. Duong AD, et al. Electrospray encapsulation of toll-like receptor agonist resiquimod in polymer microparticles for the treatment of visceral leishmaniasis. *Mol Pharm*. 2013; 10(3):1045–55. [PubMed: 23320733]
69. McConnell MJ, Hanna PC, Imperiale MJ. Adenovirus-based prime-boost immunization for rapid vaccination against anthrax. *Mol Ther*. 2007; 15(1):203–10. [PubMed: 17164792]
70. Hogenesch H. Mechanism of immunopotentiality and safety of aluminum adjuvants. *Front Immunol*. 2012; 3:406. [PubMed: 23335921]
71. Romagnani S. Th1/Th2 cells. *Inflamm Bowel Dis*. 1999; 5(4):285–94. [PubMed: 10579123]
72. Goasduff T, et al. The transcriptional response of human macrophages to murabutide reflects a spectrum of biological effects for the synthetic immunomodulator. *Clin Exp Immunol*. 2002; 128(3):474–82. [PubMed: 12067302]
73. Sridevi K, et al. Reversal of T cell anergy in leprosy patients: in vitro presentation with *Mycobacterium leprae* antigens using murabutide and Trat peptide in liposomal delivery. *Int Immunopharmacol*. 2003; 3(12):1589–600. [PubMed: 14555284]
74. Darcissac EC, et al. The synthetic immunomodulator murabutide controls human immunodeficiency virus type 1 replication at multiple levels in macrophages and dendritic cells. *J Virol*. 2000; 74(17):7794–802. [PubMed: 10933686]
75. Vidal VF, et al. Macrophage stimulation with Murabutide, an HIV-suppressive muramyl peptide derivative, selectively activates extracellular signal-regulated kinases 1 and 2, C/EBPbeta and STAT1: role of CD14 and Toll-like receptors 2 and 4. *Eur J Immunol*. 2001; 31(7):1962–71. [PubMed: 11449348]
76. McMichael AJ, Koff WC. Vaccines that stimulate T cell immunity to HIV-1: the next step. *Nat Immunol*. 2014; 15(4):319–22. [PubMed: 24646598]

77. Lofthouse S. Immunological aspects of controlled antigen delivery. *Adv Drug Deliv Rev.* 2002; 54(6):863–70. [PubMed: 12363435]
78. Cleland JL. Single-administration vaccines: controlled-release technology to mimic repeated immunizations. *Trends Biotechnol.* 1999; 17(1):25–9. [PubMed: 10098275]
79. Sivakumar SM, et al. Vaccine adjuvants - Current status and prospects on controlled release adjuvancity. *Saudi Pharm J.* 2011; 19(4):197–206. [PubMed: 23960760]
80. Hong J, et al. Inherent charge-shifting polyelectrolyte multilayer blends: a facile route for tunable protein release from surfaces. *Biomacromolecules.* 2011; 12(8):2975–81. [PubMed: 21718027]
81. Vogelhuber W, et al. Programmable biodegradable implants. *J Control Release.* 2001; 73(1):75–88. [PubMed: 11337061]
82. Feng L, et al. Pharmaceutical and immunological evaluation of a single-dose hepatitis B vaccine using PLGA microspheres. *J Control Release.* 2006; 112(1):35–42. [PubMed: 16516999]
83. DeMuth PC, et al. Implantable silk composite microneedles for programmable vaccine release kinetics and enhanced immunogenicity in transcutaneous immunization. *Adv Healthc Mater.* 2014; 3(1):47–58. [PubMed: 23847143]
84. Wang C, et al. Molecularly engineered poly(ortho ester) microspheres for enhanced delivery of DNA vaccines. *Nat Mater.* 2004; 3(3):190–6. [PubMed: 14991022]
85. Ilyinskii PO, et al. Adjuvant-carrying synthetic vaccine particles augment the immune response to encapsulated antigen and exhibit strong local immune activation without inducing systemic cytokine release. *Vaccine.* 2014; 32(24):2882–95. [PubMed: 24593999]
86. Kasturi SP, et al. Programming the magnitude and persistence of antibody responses with innate immunity. *Nature.* 2011; 470(7335):543–7. [PubMed: 21350488]
87. Kazzaz J, et al. Encapsulation of the immune potentiators MPL and RC529 in PLG microparticles enhances their potency. *J Control Release.* 2006; 110(3):566–73. [PubMed: 16360956]
88. Schlosser E, et al. TLR ligands and antigen need to be coencapsulated into the same biodegradable microsphere for the generation of potent cytotoxic T lymphocyte responses. *Vaccine.* 2008; 26(13):1626–37. [PubMed: 18295941]
89. Sahdev P, Ochyl LJ, Moon JJ. Biomaterials for nanoparticle vaccine delivery systems. *Pharm Res.* 2014; 31(10):2563–82. [PubMed: 24848341]

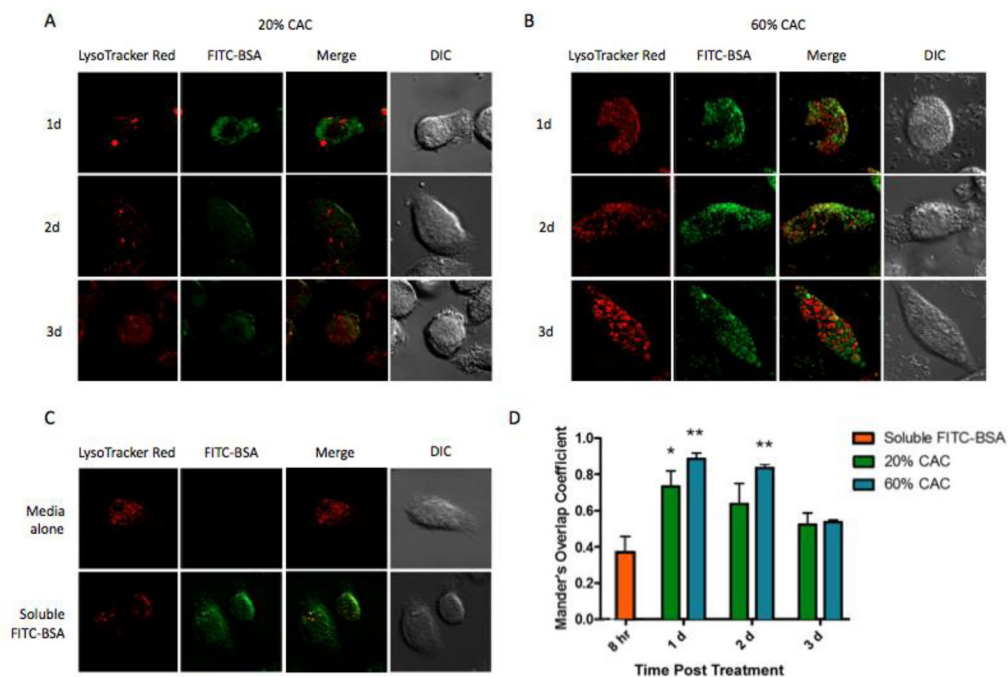




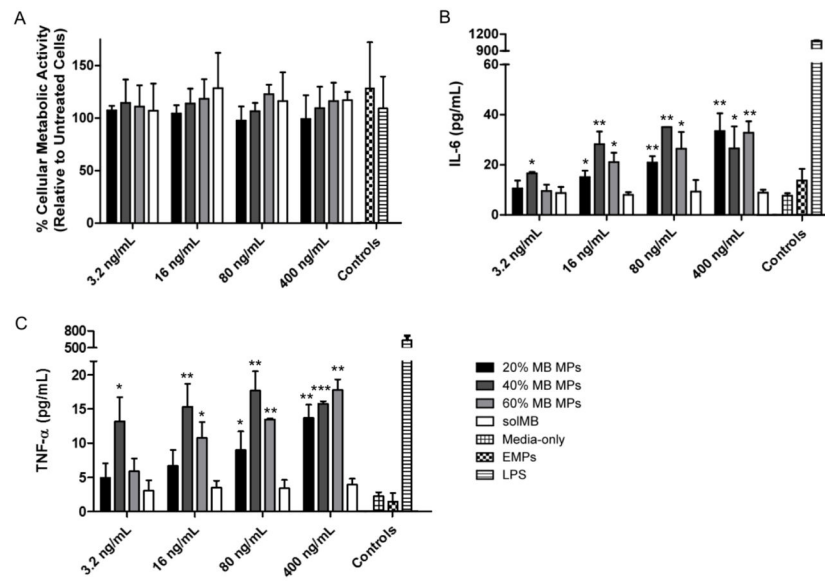
**Figure 1.** Scanning electron micrographs of (A–C) ovalbumin (OVA)-loaded and (D–F) murabutted-loaded acetalated dextran (Ace-DEX) microparticles (MPs) of different relative cyclic acetal coverage (CAC): (A, D) 20%, (B, E) 40%, and (C, F) 60%. (G) Empty MPs were fashioned from 40% Ace-DEX polymer. Scale bars are 5  $\mu\text{m}$ .



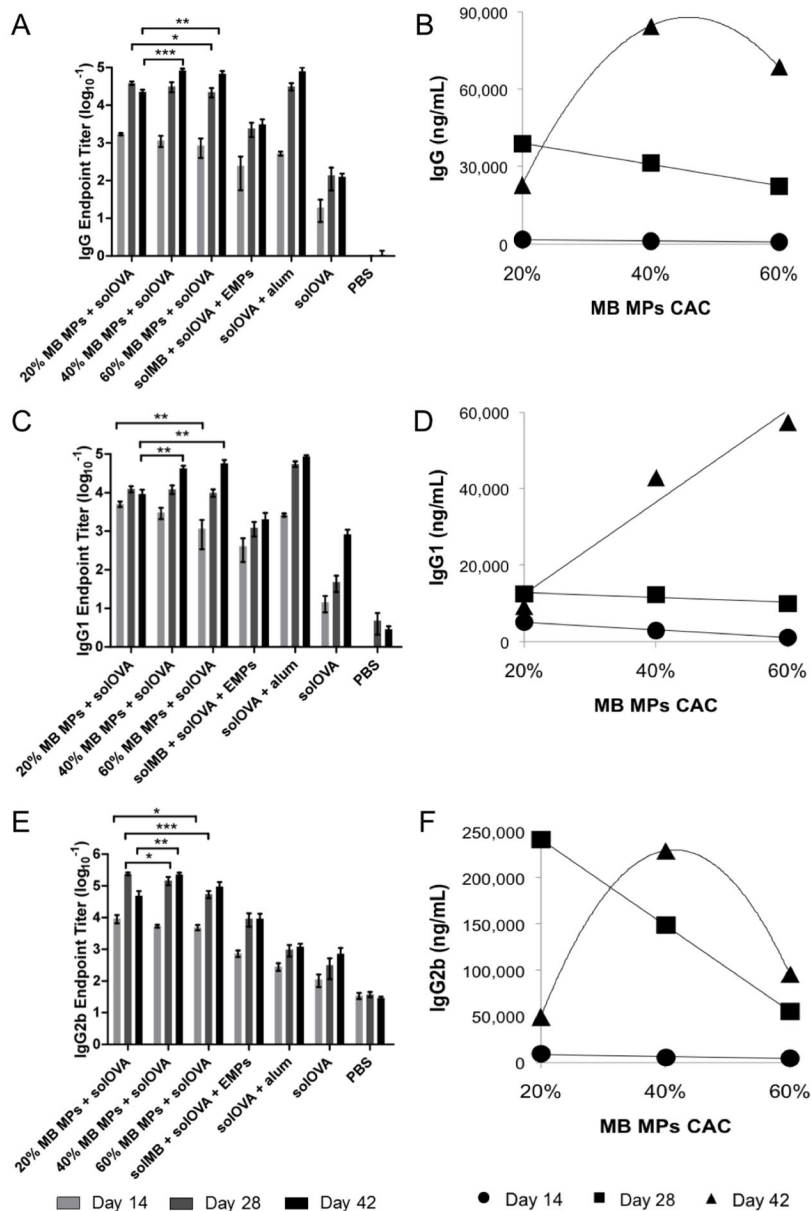
**Figure 2.** Degradation profiles of blank acetalated dextran (Ace-DEX) microparticles (MPs) of varying relative cyclic acetal coverage (CAC) at (A) pH 7.4 or (B) 6.5 at 37 °C. (C) Degradation half-lives are calculated based on 50% MP degradation. Some half-lives are reported as greater than 336 hours since less than 50% of the MPs were degraded at this final time point. Data are presented as mean ± standard deviation (n = 3).



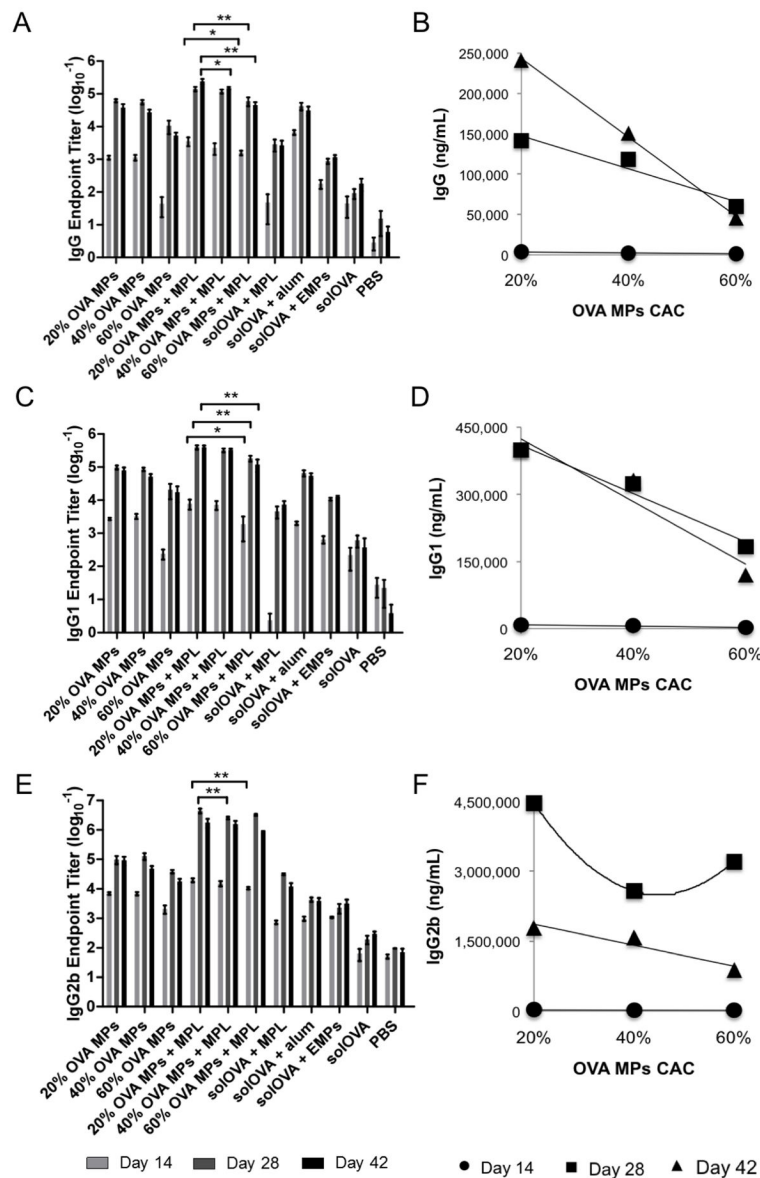
**Figure 3.** Intracellular trafficking of acetalated dextran (Ace-DEX) microparticles (MPs) containing fluorescein isothiocyanate conjugated to bovine serum albumin (FITC-BSA) within bone marrow derived dendritic cells (BMDCs). Laser scanning confocal microscopy images were obtained 1, 2, or 3 days after BMDCs were cultured with FITC-BSA MPs of (A) 20% cyclic acetal coverage (CAC) or (B) 60% CAC. (C) BMDCs were also incubated with media alone or soluble FITC-BSA for 8 hours as controls. (D) Mander's overlap coefficient was used to determine the extent of co-localization between the green (FITC-BSA) and the red (lysosome) pixels. Data are displayed as mean  $\pm$  standard error of the mean ( $n = 3$ ), and statistical significance with respect to soluble FITC-BSA is presented as \* $p < 0.05$  and \*\* $p < 0.01$ .



**Figure 4.** Innate signaling of free or encapsulated murabutide (MB) at different concentrations. (A) Cellular metabolic activity of and (B) interleukin (IL)-6 and (C) tumor necrosis factor (TNF)- $\alpha$  production by JAWSII dendritic cells after 24 hour incubation with soluble MB (solMB) or MB encapsulated within acetalated dextran (Ace-DEX) microparticles (MPs) of varying relative cyclic acetal coverage (20%, 40%, or 60 %). Empty Ace-DEX (40%) MPs (EMPs) were administered at the same concentration as that of MPs required to achieve the highest MB dose. Lipopolysaccharide (LPS, 100 ng/mL) was used as the positive control. Statistical significance with respect to solMB is presented as \* $p < 0.05$ , \*\* $p < 0.01$ , and \*\*\* $p < 0.001$ . Data are presented as mean  $\pm$  standard deviation ( $n = 3$ ).

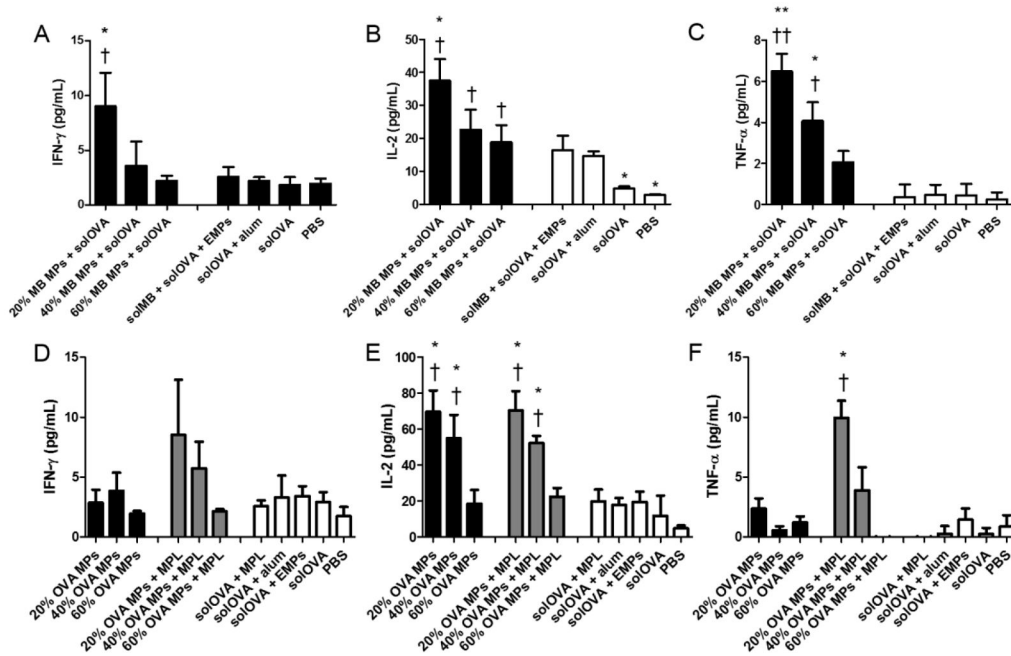


**Figure 5.** (A, B) Total IgG, (C, D) IgG1, and (E, F) IgG2b anti-ovalbumin (OVA) antibodies in mouse sera collected on Day 14, 28, and 42 post vaccination with murabutide (MB) microparticles (MPs), soluble ovalbumin (solOVA), soluble MB (solMB), empty MPs (EMPs), Alhydrogel (alum), or PBS. (B, D, F) Antibody levels for MB MPs + solOVA treatment were plotted against MP cyclic acetal coverage (CAC) with best-fitted functions as a visual guide. Data are displayed as (A, C, E) the mean logarithmic transformation (base 10) of the titers (ng/mL) ± standard error of the mean or (B, D, F) mean ± standard error of the mean (n = 8 except for Day 42 where n=4). Statistical significance between the groups of interest (MB MPs + solOVA) at various time points is presented as \*p < 0.05, \*\*p < 0.01, and \*\*\*p < 0.001.

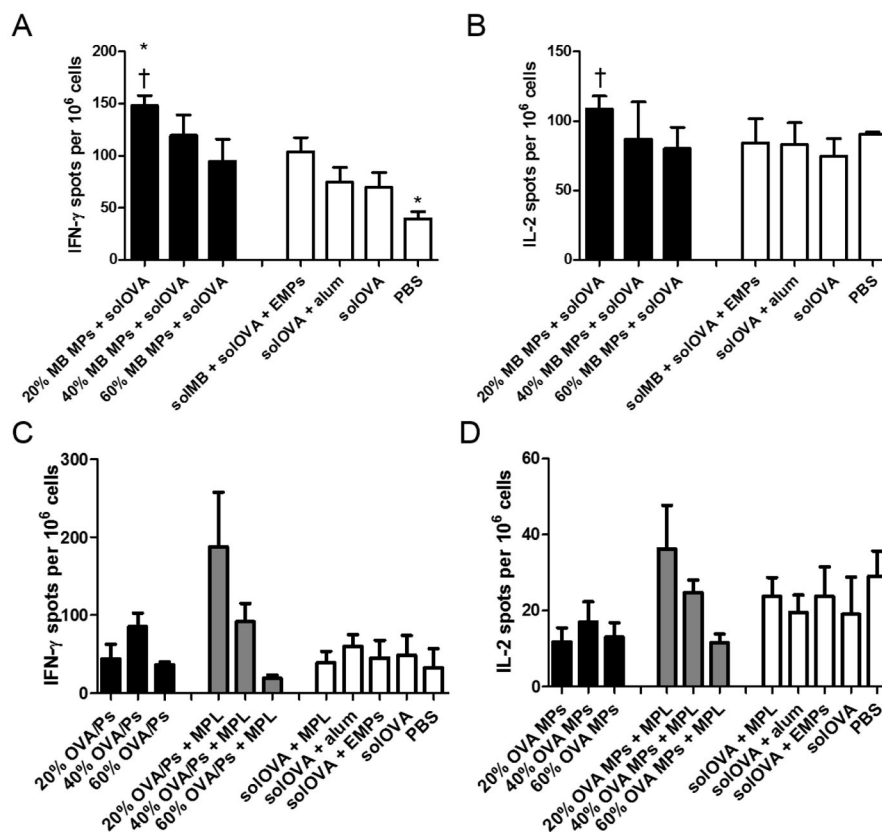


**Figure 6.** (A, B) Total IgG, (C, D) IgG1, and (E, F) IgG2b anti-ovalbumin (OVA) antibodies in mouse sera collected on Day 14, 28, and 42 post vaccination with OVA microparticles (MPs), soluble monophosphoryl lipid A (MPL), soluble OVA (solOVA), Alhydrogel (alum), empty MPs (EMPs), or PBS. (B, D, F) Antibody levels for OVA MPs + MPL treatment were plotted against MP cyclic acetal coverage (CAC) with best-fitted functions as a visual guide. Data are displayed as (A, C, E) the mean logarithmic transformation (base 10) of the titers (ng/mL) ± standard error of the mean or (D, E, F) mean ± standard error of the mean (n = 8 except for Day 42 where n=4). Statistical significance between the groups of interest (OVA MPs + MPL) at various time points is presented as \*p < 0.05 and \*\*p < 0.01.





**Figure 7.** Antigen recall measurements of (A, D) interferon (IFN)- $\gamma$ , (B, E) interleukin (IL)-2, and (C, F) tumor necrosis factor (TNF)- $\alpha$  production by splenocytes isolated from C57Bl/6 mice on Day 28 post vaccination. Mice were immunized with (A–C) murabutide (MB) microparticles (MPs), soluble ovalbumin (solOVA), soluble MB (solMB), empty MPs (EMPs), Alhydrogel (alum), or PBS, or (D–F) ovalbumin (OVA) microparticles (MPs), monophosphoryl lipid A (MPL), soluble OVA (solOVA), aluminum (alum), empty MPs (EMPs), or PBS on days 0 and 21. Statistical significance with respect to EMPs is presented as \* $p < 0.05$  and \*\* $p < 0.005$ . Statistical significance with respect to solOVA is presented as † $p < 0.05$  and †† $p < 0.005$ . Data are presented as mean  $\pm$  standard error of the mean ( $n = 4$ ).

**Figure 8.**

T-cell responses in spleens of C57Bl/6 mice measured by (A, C) interferon (IFN)-gamma ( $\gamma$ ) and (B, D) interleukin (IL)-2 ELISpot. Splenocytes were isolated on day 28 post vaccination with (A, B) murabutide (MB) microparticles (MPs), soluble ovalbumin (solOVA), soluble MB (solMB), empty MPs (EMPs), Alhydrogel (alum), or PBS, or (C, D) ovalbumin (OVA) microparticles (MPs), monophosphoryl lipid A (MPL), soluble OVA (solOVA), aluminum (alum), empty MPs (EMPs), or PBS on days 0 and 21. Statistical significance with respect to EMPs is presented as \* $p < 0.05$ . Statistical significance with respect to solOVA is presented as † $p < 0.05$ . Data are presented as mean  $\pm$  standard error of the mean ( $n = 4$ ).

**Table 1**

Summary of immunization groups testing controlled murabutide delivery.

Immunization group	MB dose ( $\mu\text{g}$ )	OVA dose ( $\mu\text{g}$ )	Alum dose ( $\mu\text{g}$ )	MP dose (mg)
Murabutide microparticles (20% cyclic acetal coverage) + soluble ovalbumin (20% MB MPs + solOVA)	5	10	-	0.51
40% MB MPs + solOVA			-	0.54
60% MB MPs + solOVA			-	0.50
soluble murabutide + solOVA + empty MPs (solMB + solOVA + EMPs)			-	0.54
solOVA + Alhydrogel (solOVA + alum)	-		250	-
solOVA	-		-	-
PBS	-	-	-	-

Author Manuscript

Author Manuscript

Author Manuscript

Author Manuscript

**Table 2**

Summary of immunization groups testing controlled ovalbumin delivery.

Immunization group	OVA dose ( $\mu\text{g}$ )	MPL dose ( $\mu\text{g}$ )	Alum dose ( $\mu\text{g}$ )	MP dose (mg)	
Ovalbumin microparticles (20% cyclic acetal coverage) (20% OVA MPs)	10	-	-	1.26	
40% OVA MPs		-	-	1.42	
60% OVA MPs		-	-	1.00	
20% OVA MPs + monophosphoryl lipid A (20% OVA MPs + MPL)		10	10	-	1.26
40% OVA MPs + MPL				-	1.42
60% OVA MPs + MPL				-	1.00
soluble OVA + MPL (solOVA + MPL)				-	-
solOVA + Alhydrogel (solOVA + alum)		-	250	-	
solOVA + empty MPs (solOVA + EMPs)		-	-	1.42	
solOVA		-	-	-	
PBS		-	-	-	-

**Table 3**

Physical characteristics of murabutide (MB)-loaded, ovalbumin (OVA)-loaded, and empty (EMPs) acetalated dextran (Ace-DEX) microparticles (MPs) of different cyclic acetal coverage (CAC). EE stands for encapsulation efficiency. Mean diameter was measured through dynamic light scattering as number-weighted average. Data are presented as mean  $\pm$  standard deviation (n = 5).

	MB-loaded Ace-DEX MPs		OVA-loaded Ace-DEX MPs		EMPs
	20	40	20	40	
Ace-DEX CAC (%)					
Compound EE (%)	98.5	92.9	79.4	70.2	99.8
Compound Loading ( $\mu\text{g agent/mg MP}$ )	9.85	9.29	7.94	7.02	9.98
Mean Diameter (nm)	604 $\pm$ 43.6	539 $\pm$ 60.9	552 $\pm$ 96.7	527 $\pm$ 110	557 $\pm$ 65.3
Endotoxin level (EU/mL)	0.047	0.063	0.027	0.044	0.081